Am J Physiol Renal Physiol 303: F790–F799, 2012.
First published June 20, 2012; doi:10.1152/ajprenal.00153.2012.

Rapid, dynamic changes in glomerular permeability to macromolecules during systemic angiotensin II (ANG II) infusion in rats

Josefin Axelsson, Anna Rippe, Carl M. Öberg, and Bengt Rippe

Department of Nephrology, Lund University, Lund, Sweden

Submitted 16 March 2012; accepted in final form 18 June 2012

Axelsson J, Rippe A, Öberg CM, Rippe B. Rapid, dynamic changes in glomerular permeability to macromolecules during systemic angiotensin II (ANG II) infusion in rats. *Am J Physiol Renal Physiol* 303: F790–F799, 2012. First published June 20, 2012; doi:10.1152/ajprenal.00153.2012.—The actions of systemic angiotensin II (ANG II) infusions on glomerular permeability were investigated in vivo. In anesthetized Wistar rats (250–280 g), the left ureter was cannulated for urine collection, while simultaneously blood access was achieved. Rats were continuously infused intravenously with either of four doses of ANG II ranging from 16 ng·kg^{-1}·min^{-1} (Lo-ANG II) to 1.82 μg·kg^{-1}·min^{-1} (Hi-ANG II), and in separate experiments with aldosterone (Aldo; 0.22 mg·kg^{-1}·min^{-1}), or with the calcium channel blocker nimodipine, or with the Aldo antagonist spironolactone together with a high ANG II dose (910 ng·kg^{-1}·min^{-1}; Hi-Int-ANG II), respectively, and with polydisperse FITC-Ficoll-70/400 (molecular radius 10–80 Å) and ^{51}Cr-EDTA. Plasma and urine samples were taken at 5, 15, 30, 60, and 120 min and analyzed by high performance size-exclusion chromatography for determination of glomerular sieving coefficients (θ) to Ficoll. Mean arterial pressure (MAP) and glomerular filtration rate (GFR) were also assessed. For ANG II, there was a rapid, marked, partly reversible increase in glomerular permeability (θ) for Ficoll molecules >34 Å in radius, peaking at 5–15 min, which was completely abrogated by the ANG II blocker candesartan but not affected by spironolactone at 15 and 30 min. For Aldo, the response was similar to that found for the lowest dose of ANG II infused. For the two highest ANG II doses given (Hi-Int-ANG II and Hi-ANG II), GFR decreased transiently, concomitant with marked, sustained increases in MAP. Nimodipine completely blocked all hemodynamic ANG II actions, whereas the glomerular permeability response remained unchanged. Thus ANG II directly increased glomerular permeability independently of its hemodynamic actions and largely independently of the concomitant Aldo response. The ANG II-induced increases in glomerular permeability were, according to a two-pore and a log-normal distributed pore model, compatible with an increased number of "large pores" in the glomerular filter, and, to some extent, an increase in the dispersity of the small-pore radius.

glomerular filtration; Ficoll; microalbuminuria; sieving coefficients; log-normal distributed pore model; aldosterone; podocytes; nimodipine; candesartan; spironolactone

THE WELL-KNOWN ANTIPROTEINURIC and renal-protective effects of ANG II converting enzyme inhibitors (ACEi) and ANG II receptor blockers (ARB) have classically been mainly assigned to renal hemodynamic effects (9, 10, 26). The present experiments were performed to investigate whether ANG II, and its secondary effector, aldosterone, can exert direct effects on glomerular permeability.[1] Of known vasoconstrictors, ANG II is one of the most potent, causing increases in mean arterial pressure (MAP) and in the glomerular filtration fraction (FF). It also induces mesangial contraction to reduce the glomerular filtration coefficient (L_pS). In addition, it releases aldosterone from the adrenal cortex, and, thereby, indirectly promotes distal nephron sodium (Na^+) reabsorption, and, at low concentrations, directly promotes Na^+ reabsorption in both proximal and distal tubules (30). Furthermore, direct effects on the glomerular permeability to macromolecules have been reported previously (15, 25, 28, 42), although the predominating view has been that increases in glomerular capillary pressure may be the main reason for its effect to increase the glomerular filtration of proteins. However, it is now well established that the podocytes in the glomerular filtration barrier (GFB) are contractile and dynamically active (1, 22, 25, 42, 44). Both podocytes and endothelial cells have ANG II receptors (mainly AT1R), and it was earlier reported that ANG II can induce cytoskeletal changes involving the F-actin cytoskeleton in cultured podocytes (44). The F-actin pattern thus changed from a random to a more stellate pattern after ANG II exposure, with reduced peripheral F-actin staining, conceivably indicating F-actin fiber contraction. In a more recent study, ANG II induced membrane "ruffling" and loss of stress fibers in podocytes (22). A recent review has summarized the tentative mechanisms whereby ANG II, after binding to its receptor, can induce cellular Ca^{2+} influx via so-called transient receptor potential canonical (TRPC) channels, TRPC5 and, to some extent, TRPC6, to modulate the actin cytoskeleton in podocytes, involving, among other things, downstream interactions with calcineurin, protein kinase A (PKA), synaptopodin, nuclear factor of activated T-cells (NFAT), and small GTPases (Rac1, Cdc42, and RhoA) (17).

Despite many indications that ANG II may affect glomerular permeability by direct actions on the GFB, some studies have indicated that the renin-angiotensin-aldosterone-system (RAAS) may not have specific effects on glomerular permeability at all. In the isolated, perfused kidney, the increases in fractional clearance for albumin after ANG II were correlated neither with renal hemodynamic changes nor with glomerular permeability alterations, as indicated from the fractional glomerular clearance (sieving coefficient; θ) of Ficoll of a 36-Å radius ($Ficoll_{36Å}$) or IgG (13). Indeed, there is an ongoing controversy, whether normal glomeruli are highly permeable to macromolecules and filter nephrotic levels of albumin (14, 41), or if they show a very high selectivity to albumin according to the classic view (12, 19). Micropuncture studies (15, 48) and glomerular sieving data for high-molecular-weight FITC-Ficoll and albumin in vivo (4–6), and recent results from in vivo two-photon excitation microscopy (34, 46), unequivocally support the notion of a very tight GFB, demonstrating a θ to albumin on the order of only 1×10^{-4} (19).

In view of the controversial effects of ANG II, and its secondary effector, aldosterone, on the functional behavior of

[1] This article is the topic of an Editorial Focus by Fredrik Palm (31a).

Address for reprint requests and other correspondence: B. Rippe, Dept. of Nephrology, Lund Univ., Univ. Hospital of Lund, S-211 85 Lund, Sweden (e-mail: Bengt.Rippe@med.lu.se).

the GFB, we decided to investigate their actions on glomerular permeability in rats in vivo using the assessment of glomerular sieving coefficients for FITC-Ficoll 70/400 (M_r ~70,000 and ~400,000, respectively). Ficoll is a neutral polysaccharide, which is not significantly reabsorbed by proximal tubules, and allows the determination of θ, i.e., the filtrate-to-plasma concentration ratios, for a broad spectrum of molecular radii (13–80 Å). In the present study emphasis was on the glomerular sieving pattern of Ficoll molecules of high molecular weight (M_r ~400,000). A rapid, partly reversible and dose-dependent increase in glomerular permeability, completely abrogated by candesartan, was noted for ANG II. The effects were unchanged even when the vasoconstrictive actions of ANG II were completely abolished by simultaneously administering the L-type calcium channel blocker nimodipine.

METHODS

Animals and general surgery. Experiments were performed in 56 male Wistar rats (Möllegard, Lille Stensved, Denmark) with an average body weight of 265.9 ± 1.7 g. The rats had free access to standard food and water until the day of the experiment. The animal Ethics Committee at Lund University approved the experiments. Anesthesia was induced by an intraperitoneal injection of pentobarbital sodium (60 mg/kg body wt) and maintained through repeated intra-arterial injections of the same drug. The rats were placed on a heating pad to maintain body temperature at 37°C. A tracheotomy was performed to facilitate breathing. The tail artery was cannulated (PE-50 cannula) for continuous monitoring of blood pressure and heart rate on a polygraph (model 7B; Grass Instruments, Quincy, MA), and for administration of anesthesia. The left carotid artery and left and right jugular veins were cannulated (PE-50) for blood sampling and infusions, respectively. Access to the left urether was obtained through a small (6–8 mm) abdominal incision. Furosemide (0.375 mg/kg, Furosemid, Recip, Sweden) was administered in the tail artery to increase urine production and facilitate cannulation of the urether, used for urine sampling. The urether was dissected free, and a PE-10 (connected to a PE-50) cannula was inserted and secured by a ligature.

Experimental procedures: systemic intravenous infusions of ANG II. All experiments started with an initial rest period of 20 min following the cannulation of the left urether. Immediately after the rest period, sampling of urine and plasma for Ficoll-sieving measurements was performed during a 5-min control ("baseline") period before the start of the infusion of ANG II (A9525, Sigma-Aldrich) at *time 0*. After the start of the infusion, sequential measurements of the effects of ANG II on glomerular permeability were done at 5, 15, 30, 60, and 120 min. ANG II was given as a bolus dose followed by a continuous infusion throughout the experiment. Four different doses of ANG II were given: either a low dose (Lo-ANG II, $n = 7$; a bolus dose of 50 ng followed by a continuous infusion of 16.2 ng·kg^{-1}·min^{-1}) a low intermediate dose (Lo-Int-ANG II, $n = 8$; a bolus dose of 1.09 μg followed by a continuous infusion of 230 ng·kg^{-1}·min^{-1}), a high intermediate dose (Hi-Int-ANG II, $n = 7$; a bolus dose of 4.38 μg followed by continuous infusion of 910 ng·kg^{-1}·min^{-1}), or a high dose of ANG II (Hi-ANG II, $n = 8$; and a bolus dose of 8.75 μg followed by continuous infusion of 1.82 μg·kg^{-1}·min^{-1}). The Lo-ANG II group was chosen to yield a slightly elevated ANG II plasma concentration compared with normal (2×10^{-10} M) (11). The two highest levels (Hi-Int-ANG II and Hi-ANG II) represent ANG II concentrations compatible with the situation prevailing in malignant hypertension (11). One separate group of animals received the L-type Ca^{2+} channel blocker, nimodipine (0.3 μg·kg^{-1}·min^{-1}, Nimotop, Bayer, Solna, Sweden) together with the Hi-Int-ANG II dose (Nim-Hi-Int-ANG II; $n = 6$) to investigate the impact of ANG II on the glomerular barrier when the ANG II hemodynamic effects are totally blocked. Yet another separate group was infused with aldosterone ($n = 7$; A9477, Sigma-Aldrich). An initial bolus (0.6 mg) was followed by a continuous infusion of 0.22 mg·kg^{-1}·min^{-1} of aldosterone. This dose is fourfold higher than that calculated to yield circulating aldosterone concentrations within the physiological range (38) and about twice the concentration resulting from the lowest dose of ANG II infused in the present study (21). One group of ANG II-infused animals received a single intravenous (iv) dose of the aldosterone antagonist spironolactone (Spir-Hi-Int-ANG II, $n = 7$, 20 mg/kg; Soldactone, Pfizer, Sollentuna, Sweden) 15 min before administration of ANG II in the Hi-Int-ANG II dose. In one group of animals, the AT1R antagonist candesartan (Cand-Hi-Int-ANG II, $n = 6$, 0.2 mg/kg; a gift from Astra-Zeneca, Mölndal, Sweden) was administered iv as a single dose 15 min before the start of the Hi-Int-ANG II dose infusion. The Cand-Hi-Int-ANG II group was followed for 15 and 30 min.

Sieving of FITC-Ficoll. A mixture of FITC-Ficoll-70 (10 mg/ml) and FITC-Ficoll-400 (10 mg/ml; TdB Consultancy, Uppsala, Sweden), in a 1:24 relationship together with FITC-inulin (10 mg/ml; TdB Consultancy) was used. The bolus dose (FITC-Ficoll-70, 40 μg; FITC-Ficoll-400, 960 μg; and FITC-inulin, 500 μg) was followed by a constant infusion of 10 ml·kg^{-1}·h^{-1} (FITC-Ficoll-70, 20 μg/ml; FITC-Ficoll-400, 0.48 mg/ml; FITC-inulin, 0.5 mg/ml; and ^{51}Cr-EDTA, 0.3 MBq/ml) for at least 20 min before sieving measurements, after which urine from the left kidney was collected for 5 min, with a midpoint (2.5 min) plasma sample collected.

Plasma and urine samples were assessed for concentrations for FITC-Ficoll on a high-performance size exclusion chromatography (HPSEC) system (Waters, Milford, MA) using a Ultrahydrogel 500 column (with guard column, Waters) and calibrated as described in detail elsewhere (3). The mobile phase was driven by a pump (Waters 1525), and fluorescence was detected with a fluorescence detector (Waters 2475) with an excitation wavelength set at 492 nm and an emission wavelength at 518 nm. The samples were loaded to the system with an autosampler (Waters 717 plus). The system was controlled by Breeze Software 3.3 (Waters). The glomerular θ is defined as the filtrate-to-plasma concentration ratio, i.e., the concentration of solute in the primary urine over that in plasma. Ficoll θ values were obtained by analyzing the HPLC curves, i.e., Ficoll concentration vs. elution time (the relative distribution volumes of the different size Ficoll molecules in the column) from the plasma and urine samples for each experiment. The urine Ficoll concentration (Cu_{Ficoll}) vs. the a_e curve divided by that of the plasma Ficoll concentration (Cp_{Ficoll}) vs. a_e relationship was divided by the urine inulin-to-plasma concentration ratio (Cu_{in}/Cp_{in}) to obtain the primary urine (ultrafiltrate) concentration of Ficoll for every a_e. Hence

$$\theta = \frac{Cu_{Ficoll}}{Cp_{Ficoll}} \times \frac{Cp_{in}}{Cu_{in}}$$

Glomerular filtration rate. The glomerular filtration rate (GFR) was measured in the left kidney during the experiment, using ^{51}Cr-EDTA. A priming dose of ^{51}Cr-EDTA (0.3 MBq in 0.2 ml iv, Amersham Biosciences, Buckinghamshire, UK) was administered and followed by a continuous infusion (10 ml·kg^{-1}·h^{-1}) of ^{51}Cr-EDTA (0.37 MBq/ml in 0.9% NaCl) throughout the experiment. Urine was collected from the left urether repeatedly during the experiment, and blood samples, using microcapillaries, were taken for calculation of GFR, approximately every 10–30 min. Radioactivity in blood and urine was measured in a gamma counter (Wizard 1480, Wallac, Turku, Finland). Hematocrit was assessed throughout the experiments to be able to convert blood radioactivity into plasma radioactivity. During the FITC-Ficoll sieving period, GFR was also assessed from the urine clearance of FITC-inulin (results not shown). GFR was calculated by dividing the urinary excretion ($U_t \times V_u$) of ^{51}Cr-EDTA and inulin per minute with the plasma tracer concentration (P_t). U_t represents the tracer concentration in urine, and V_u the flow of urine per minute.

Two-pore analysis. A two-pore model (27, 39) was used to analyze the θ data for Ficoll (molecular radius 10–80 Å). A nonlinear least-squares regression analysis was used to obtain the best curve fit, using scaling multipliers, as described at some length previously (40). The four major parameters of the two-pore model are the small-pore radius (r_s), the large-pore radius (r_L), the unrestricted pore area over unit diffusion path-length ($A_0/\Delta X$), and the fraction of the glomerular UF coefficient accounted for by the large pores (α_L).

Log-normal distributed+shunt model. A log-normal distributed+shunt model was also employed to analyze the θ data for Ficoll as a function of a_e, as described at some length in APPENDIX 1.

Statistics. Values are represented as means ± SE. Statistical differences between test period results and those obtained during control conditions before drug infusions (baseline) were tested by nonparametric analysis, using a Kruskal-Wallis test followed by post hoc testing using a Mann-Whitney *U*-test. Bonferroni corrections for multiple comparisons were made. Significance levels were set at $*P < 0.05$, $**P < 0.01$, and $***P < 0.001$. All statistical calculations were made using SPSS 18.0 for Windows (SPSS, Chicago, IL).

RESULTS

Lo-ANG II, Lo-int-ANG II. Figure 1*A* shows the glomerular sieving curves, i.e., the glomerular θ plotted vs. the Stokes-Einstein radius (a_e), for Ficoll molecules ranging from 10 to 80 Å in radius assessed at 15 min after the start of the ANG II infusion for moderately supraphysiological (Lo-ANG II) and high supraphysiological (Lo-Int-ANG II) ANG II doses. A rapid, marked increase in θ for large Ficoll molecules ($Ficoll_{50-80Å}$) was seen for both groups compared with baseline. Furthermore, the small pore radius was slightly, but significantly increased (compared with baseline) in the Lo-Int-ANG II group (Table 1). θ for $Ficoll_{70Å}$ increased rapidly and reversibly as a function of time, the increase peaking at 5–15 min, as shown in Fig. 1*B*, while there were no significant alterations in the GFR, as shown in Fig. 1*C*. However, for the Lo-Int-ANG II group there was an increase in mean arterial pressure (MAP), as shown in Table 2. Thus MAP for the Lo-Int-ANG II started to increase immediately after the start of the ANG II infusion to remain high throughout the experiment.

Hi-ANG II, Hi-Int-ANG II. Figure 2*A* shows the glomerular sieving curves (θ vs. a_e) for Ficoll at 15 min for the two high doses of ANG II infusion. The changes in the sieving curves reflect both a dose-dependent increase in fluid flow through the large-pore system (Jv_L/GFR) and an increase in the small-pore radius for Hi-Int-ANG II and Hi-ANG II, respectively, according to the two-pore model (Table 1). Figure 2*B* demonstrates a rapid, marked glomerular permeability increase, with an early, large permeability peak vs. baseline at 5 and 15 min, partly reversible within 30 min. Thus θ for $Ficoll_{70Å}$ increased from $1.98 \times 10^{-5} \pm 6.75 \times 10^{-6}$ to $2.66 \times 10^{-4} \pm 5.03 \times 10^{-5}$ ($P < 0.01$) and from $3.89 \times 10^{-5} \pm 5.57 \times 10^{-6}$ to $5.41 \times 10^{-4} \pm 1.25 \times 10^{-4}$ ($P < 0.01$) at 15 min for Hi-Int-ANG II and Hi-ANG II, respectively. After 30 min there was a more sustained increase in θ for $Ficoll_{70Å}$, maintained over 2 h for the two groups. Figure 2*C* illustrates that, unlike the situation for the two lower ANG II doses, there was a marked initial and transient reduction in GFR for the highest doses of ANG II given. For Hi-Int-ANG II and Hi-ANG II, GFR at 5 min thus decreased from 0.73 ± 0.08 to 0.32 ± 0.05 $ml \cdot min^{-1} \cdot g\ (kidney)^{-1}$ ($P < 0.01$) and from 0.64 ± 0.03 to 0.21 ± 0.07 $ml \cdot min^{-1} \cdot g\ (kidney)^{-1}$ ($P < 0.01$), respectively. For the two highest doses of ANG II infused, there were rapid, marked

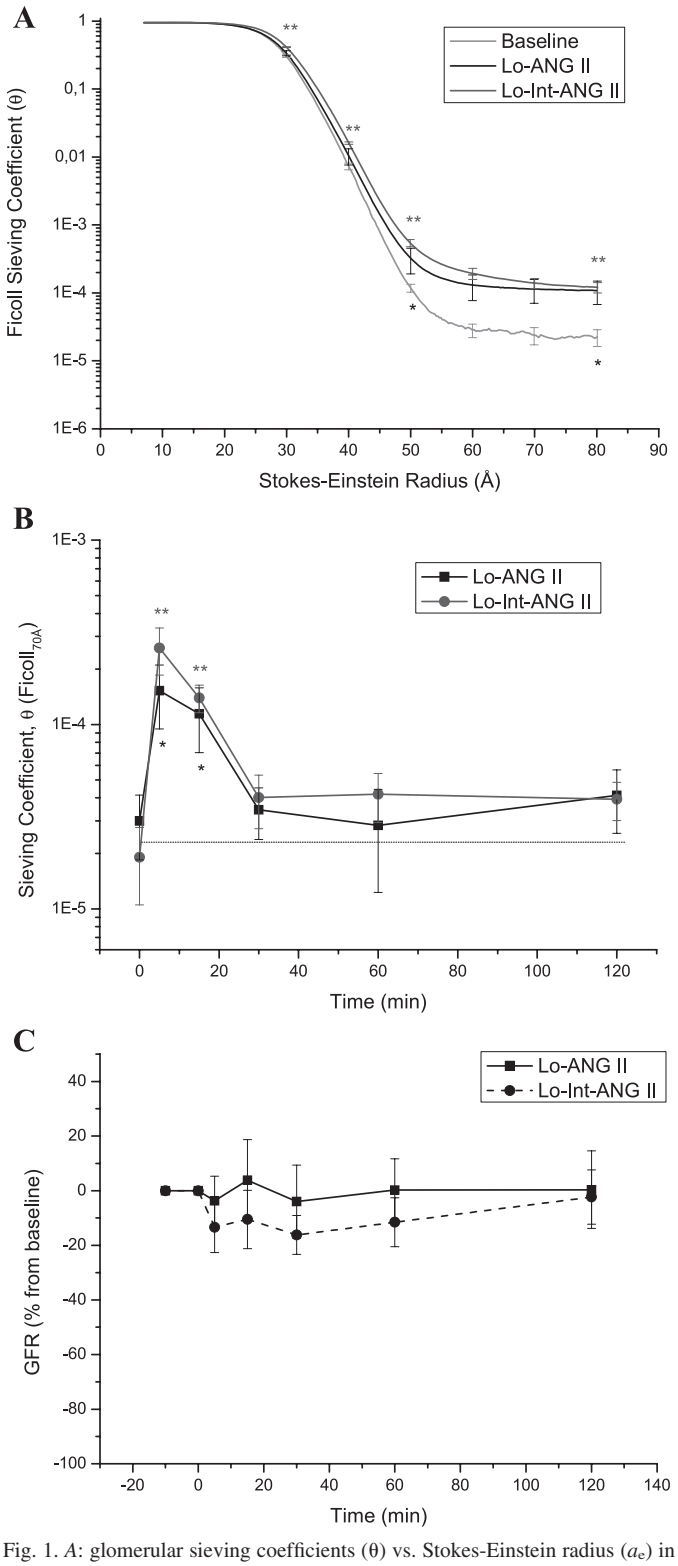

Fig. 1. *A*: glomerular sieving coefficients (θ) vs. Stokes-Einstein radius (a_e) in Lo-ANG II and Lo-Int-ANG II vs. baseline. In Lo-ANG II, there was a significant increase in θ for $Ficoll_{50-80Å}$ ($P < 0.05$). In Lo-Int-ANG II, there was also an increased θ for Ficoll of 30- to 50-Å radius ($P < 0.05$). *B*: θ for $Ficoll_{70Å}$ vs. time for Lo-ANG II and Lo-Int-ANG II vs. the combined baseline values for the 2 doses. There was a marked increase in θ already at 5 min for both groups, partly reversible within the next 20–60 min. Symbols and lines are as in *A*. *C*: glomerular filtration rate (GFR) as a function of time (% of baseline value) for Lo-ANG II (solid line) and Lo-Int-ANG II (dashed line). There were no significant changes in GFR over time for these 2 ANG II doses.

Table 1. *Two-pore parameters for Lo-ANG II, Lo-Int-ANG II, Hi-Int-ANG II, and Hi-ANG II at 15 and 120 min*

	Baseline	Lo-ANG II 15 min	Lo-ANG II 120 min	Lo-Int-ANG II 15 min	Lo-Int-ANG II 120 min	Hi-Int-ANG II 15 min	Hi-Int-ANG II 120 min	Hi-ANG II 15 min	Hi-ANG II 120 min
Small-pore radius (r_s), Å	45.1 ± 0.29	44.8 ± 0.65	44.7 ± 0.20	45.9 ± 0.10†	44.9 ± 0.28	46.5 ± 0.13†	46.2 ± 0.16*	47.8 ± 0.14*	47.0 ± 0.13
Large-pore radius (r_L), Å	120 ± 5.21	164 ± 15.4	131 ± 12.5	154 ± 15.1	131 ± 9.23	121 ± 9.37	130 ± 9.86	107 ± 4.80	139 ± 9.96
$\alpha_L \times 10^5$	4.07 ± 0.51	6.53 ± 2.98	2.63 ± 0.32	11.5 ± 2.81†	3.93 ± 0.57	53.7 ± 14.2†	18.8 ± 2.76†	134 ± 43.4†	14.3 ± 2.3*
Jv_L/GFR $\times 10^5$	13.1 ± 2.04	20.9 ± 9.16	9.98 ± 2.47	33.9 ± 7.77	11.3 ± 1.61	145 ± 36.1†	51.7 ± 9.53†	328 ± 96.6†	42.8 ± 7.71*
$A_0/\Delta X$, cm/g $\times 10^{-5}$	6.73 ± 0.35	7.92 ± 0.40	6.44 ± 0.13*	7.28 ± 0.85	7.08 ± 0.55	6.74 ± 0.57	6.33 ± 0.13	3.69 ± 0.38	4.40 ± 0.33

Values are means ± SE. Baseline represents the pooled baseline data from all groups. See text for further definitions of groups. r_s, Small-pore radius; r_L, large-pore radius; α_L, fractional ultrafiltration coefficient accounted for by large pores; Jv_L/GFR, fractional fluid flow through large pores; GFR, glomerular filtration rate; $A_0/\Delta X$, effective pore area over unit diffusion path-length. Statistical differences between experimental groups and baseline: *$P < 0.05$, †$P < 0.01$.

increases in MAP, which were sustained over the entire experiment. MAP, heart rate, and hematocrit are shown in Table 2.

Aldosterone. Figure 3*A* shows the glomerular sieving curves (θ vs. a_e) for Ficoll molecules ranging from 10 to 80 Å in radius assessed at 15 min after the start of the aldosterone infusion (0.22 mg·kg^{-1}·min^{-1}). A rapid increase in θ for large Ficoll molecules ($Ficoll_{50-80Å}$), but not for small ones ($Ficoll_{10-50Å}$), was seen at 5 and 15 min compared with baseline in a fashion very similar to what was found for low doses of ANG II (Lo-ANG II). Thus the early increase in θ for $Ficoll_{70Å}$ was largely reversible within 30 min (Fig. 3*B*). Despite the initial increases in θ for $Ficoll_{70Å}$, two-pore parameters did not change significantly (data not shown). No changes in GFR (Fig. 4*B*), MAP, heart rate, or hematocrit (Table 5) were noted over 2 h (cf. Lo-ANG II).

Effects of candesartan, nimodipine, and spironolactone in Hi-Int-ANG II. Figure 4*A* shows θ for $Ficoll_{70Å}$ as a function of time for Hi-Int-ANG II alone, or in Hi-Int-ANG II together with either candesartan, nimodipine, or spironolactone. Candesartan totally blocked all actions of ANG II on glomerular permeability and renal hemodynamics, as indicated by the unchanging θ ($Ficoll_{70Å}$), GFR, and MAP over time (Fig. 4*A* and Table 5). Furthermore, totally blocking the hemodynamic actions of ANG II, by coadministering nimodipine in Hi-Int-ANG II, did not affect angiotensin's marked effect on glomerular permeability. Thus the increase in θ for $Ficoll_{70Å}$ was from $2.25 \times 10^{-5} \pm 5.94 \times 10^{-6}$ to $4.42 \times 10^{-4} \pm 1.26 \times 10^{-4}$ at 15 min in the Nim-Hi-Int-ANG II group. Pretreating the animals in Hi-Int-ANG II with spironolactone (Spir-Hi-Int-ANG II) nearly completely blocked the permeability effects of ANG II at 60 and 120 min but did not affect the permeability actions of ANG II at 15 and 30 min, even though the very early, rapid (within 5 min) response to ANG II was slightly blunted. Data for MAP, heart rate, and hematocrit in animals treated with high intermediate doses of ANG II together with either candesartan, nimodipine, or spironolactone are shown in Table 5, while the two-pore parameters for Nim-Hi-Int-ANG II and Spir-Hi-Int-ANG II are listed in Tables 3 and 4, respectively. Spironolactone did not affect the vasoconstriction induced by ANG II (Hi-Int-ANG II), but despite that, it prevented the initial dip in GFR. In Spir-Hi-Int-ANG II, MAP increased from 113.3 ± 3.6 to 144.2 ± 2.4 mmHg ($P < 0.01$) at 5 min after the start of the ANG II infusion and remained elevated throughout the experiment (Table 5).

Two-pore parameters. The best curve fits of θ vs. a_e for Ficoll according to the two-pore model were obtained using the parameters listed in Tables 1, 3, and 4, for the different experimental groups investigated at 15 and 120 min. The fractional hydraulic conductance accounted for by the large pores (α_L) increased in Lo-Int-ANG II, Hi-Int-ANG II and Hi-ANG II compared with control ($P < 0.01$) at 15 min and for Hi-Int-ANG II ($P < 0.01$) and for Hi-ANG II at 120 min ($P < 0.05$), indicating the formation of more large pores in the glomerular filter during the ANG II infusion. Similarly, the fractional fluid flow through the large pores (Jv_L/GFR) was also increased in Hi-Int-ANG II and Hi-ANG II at both 15 and 120 min. Furthermore, there was an increase in small-pore radius (r_s) at 15 min for Lo-Int-ANG II and Hi-Int-ANG II. As

Table 2. *Mean arterial pressure (MAP), heart rate (HR), and hematocrit in the 4 ANG II groups*

	Baseline	5 min	15 min	30 min	60 min	120 min
Lo-ANG II, $n = 7$						
Hct, %	49.3 ± 0.6	49.8 ± 1.2	47.6 ± 0.6	47.4 ± 0.5*	46.1 ± 0.5*	46.1 ± 0.6*
MAP, mmHg	107 ± 2.1	109 ± 2.4	110 ± 2.3	109 ± 2.2	109 ± 2.3	108 ± 2.8
HR, beats/min	335 ± 17	347 ± 27	333 ± 23	334 ± 16	320 ± 22	320 ± 20
Lo-Int-ANG II, $n = 8$						
Hct, %	48.6 ± 0.4	50.1 ± 0.5	50.3 ± 0.5	49.7 ± 0.7	49.3 ± 0.6	48.9 ± 0.9
MAP, mmHg	122 ± 4.5	148 ± 3.1†	147 ± 3.0†	146 ± 3.9†	144 ± 5.3*	144 ± 4.4*
HR, beats/min	377 ± 13	381 ± 11	382 ± 13	382 ± 12	365 ± 9	362 ± 10
Hi-Int-ANG II, $n = 7$						
Hct, %	48.9 ± 0.5	50.0 ± 0.5	49.8 ± 0.4	50.1 ± 0.4	50.4 ± 0.5	50.3 ± 0.7
MAP, mmHg	123 ± 4.5	158 ± 2.5†	156 ± 1.9†	156 ± 2.9†	153 ± 2.1†	150 ± 2.2†
HR, beats/min	387 ± 14	389 ± 13	383 ± 9	373 ± 23	377 ± 13	375 ± 13
Hi-ANG II, $n = 8$						
Hct, %	48.8 ± 0.7	50.5 ± 0.8	50.5 ± 0.7	50.3 ± 0.9	49.2 ± 0.6	48.3 ± 1.2
MAP, mmHg	108 ± 5.6	141 ± 5.2‡	139 ± 5.2‡	137 ± 3.8‡	137 ± 2.9‡	136 ± 2.5‡
HR, beats/min	354 ± 12	350 ± 14	353 ± 15	340 ± 20	335 ± 12	337 ± 11

Values are means ± SE. Statistical differences between experimental groups and baseline: *$P < 0.05$, †$P < 0.01$, ‡$P < 0.001$.

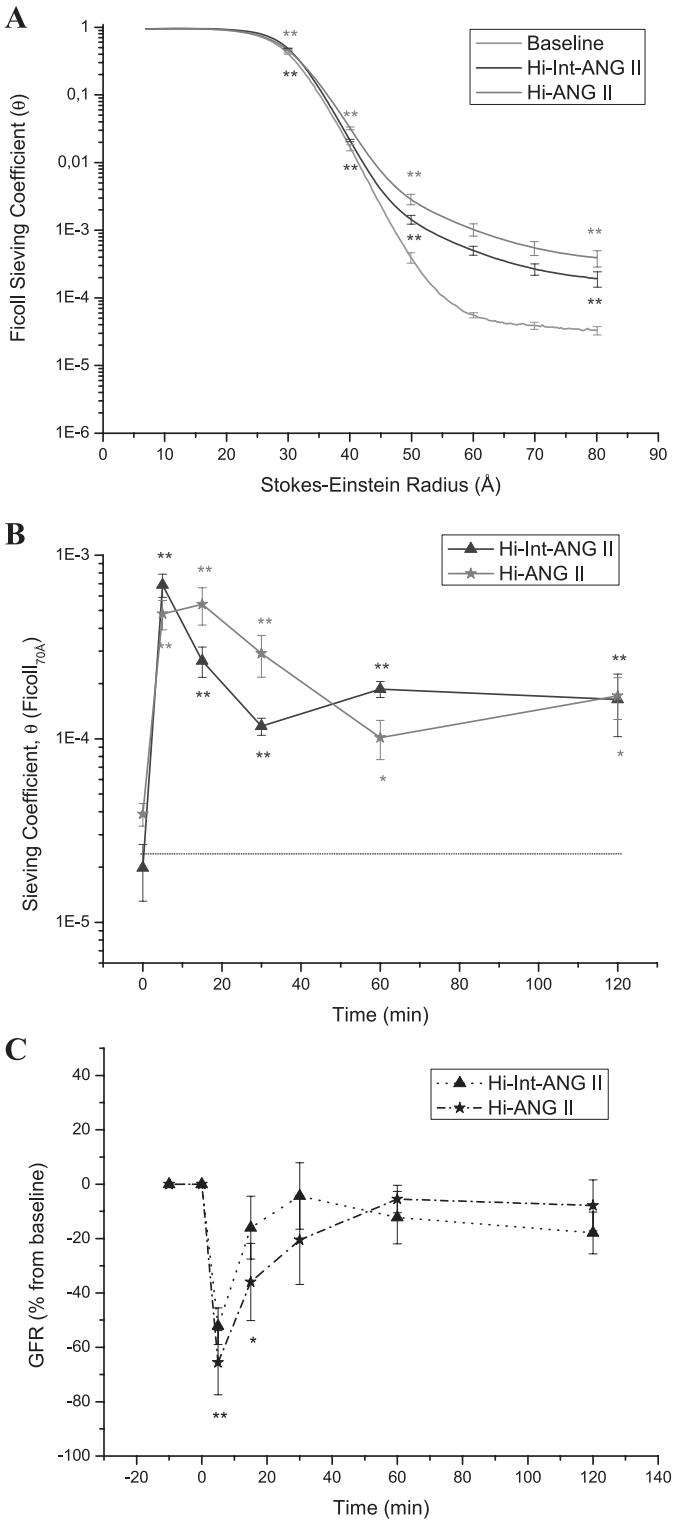

Fig. 2. *A*: θ vs. a_e in Hi-Int-ANG II and Hi-ANG II vs. baseline (pooled for the 2 groups). There was a significant increase in θ for a_e ranging from 30 to 80 Å for both Hi-Int-ANG II and Hi-ANG II. *B*: θ for $Ficoll_{70Å}$ vs. time for Hi-Int-ANG II and Hi-ANG II. There was a rapid, marked increase in θ already at 5 min for the 2 groups, only partly reversible within the next 20–60 min. Glomerular permeability was still markedly enhanced (by an order of magnitude) at 2 h. Symbols and lines are as in *A*. *C*: GFR as a function of time (% of baseline value) for the highest doses of ANG II infusion. Dotted line, Hi-Int-ANG II; dashed-dotted line, Hi-ANG II. A transient, marked initial dip in GFR was seen for the 2 highest ANG II doses, largely reversed within 40–60 min.

in the Hi-Int-ANG II group, Nim-Hi-Int-ANG II showed an increase in both α_L and in Jv_L/GFR similar to the Spir-Hi-Int-ANG II group. The unrestricted pore area over unit diffusion path length ($A_0/\Delta X$) was found to be stable during the experiments, except for a reduction at 5 min (results not shown) for Hi-Int-ANG II and Hi-ANG II, concomitant with the initial reduction in GFR in these groups, which may reflect a reduction in the glomerular filtration coefficient (L_pS).

Log-normal distributed+shunt model. Results from applying the log-normal distributed pore+shunt model to Ficoll θ vs. a_e data are shown for Lo-ANG II and Hi-Int-ANG II at 15 and 120 min, respectively, vs. baseline data (for the Hi-Int-ANG II group) in Table 6. The average small-pore radius (u) was reduced for the two highest ANG II doses compared with control at both 15 and 120 min ($P < 0.01$), while the distribution parameter of the pore radius (s) was seen to increase (at both these time points) for the Hi-Int-ANG II ($P < 0.01$). This occurred in parallel with an increase in the fluid flow through the shunt-pathway, with the highest value found at 15 min ($P < 0.01$).

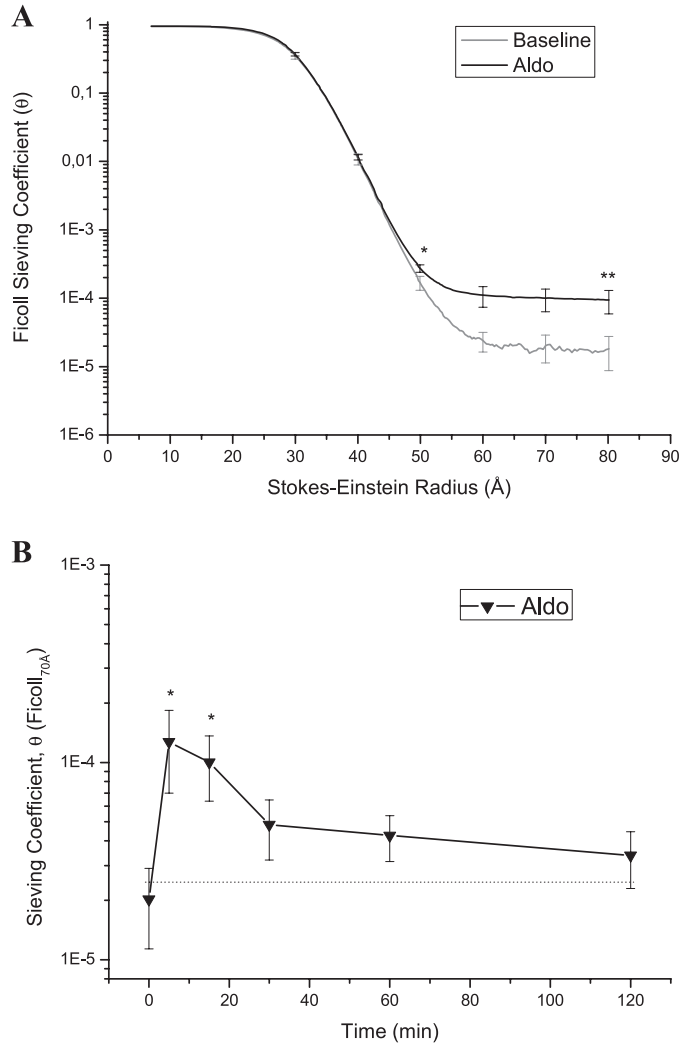

Fig. 3. *A*: θ vs. a_e for aldosterone (Aldo; 0.22 $mg \cdot kg^{-1} \cdot min^{-1}$). There was a significant increase in θ for $Ficoll_{50-80Å}$ with no change in θ for Ficoll molecules <50 Å in radius. *B*: θ for $Ficoll_{70Å}$ vs. time in animals receiving systemic Aldo infusion. There was a rapid, reversible increase in glomerular permeability for Aldo, similar to that shown for Lo-ANG II.

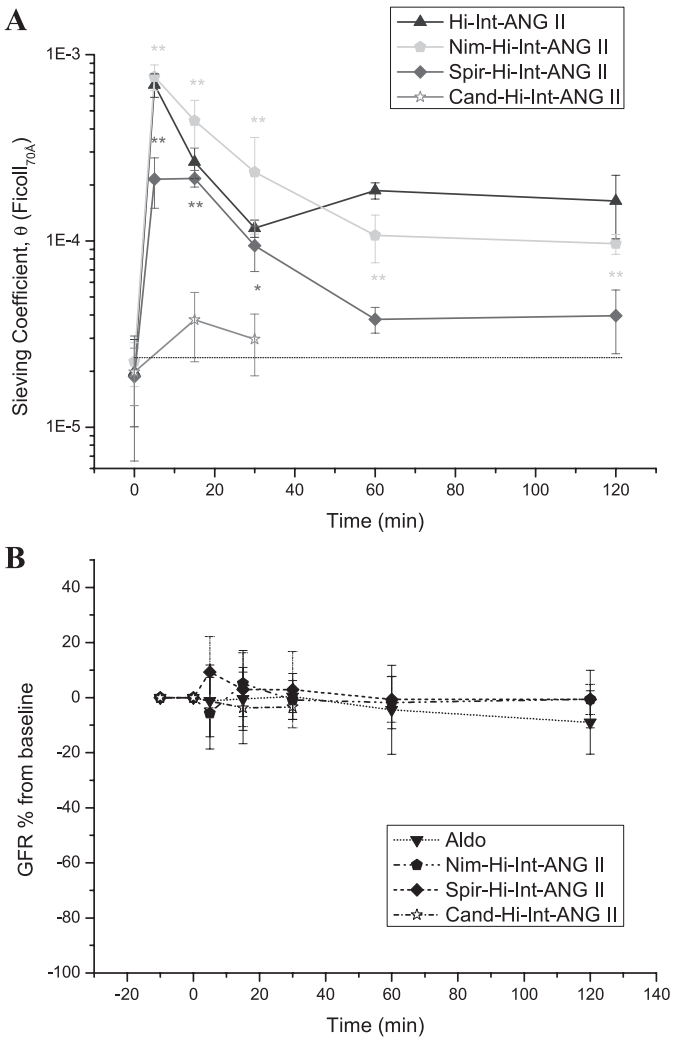

Fig. 4. *A*: θ as a function of time for $Ficoll_{70Å}$ in groups receiving the Hi-Int-ANG II dose together with either candesartan (Cand-Hi-Int-ANG II), nimodipine (Nim-Hi-Int-ANG II), or spironolactone (Spir-Hi-Int-ANG II) vs. Hi-Int-ANG II alone (Hi-Int-ANG II). The horizontal line represents nonstimulated animals (for the baseline period in the Hi-Int-ANG II group). Note that nimodipine, which completely abrogated the hemodynamic actions of ANG II, did not significantly affect the permeability effects in Hi-Int-ANG II. Spironolactone significantly inhibited the effects of Hi-ANG II at 60 and 120 min, but not at 15 and 30 min. *B*: GFR as a function of time (% of baseline value) in the groups receiving ANG II (Hi-Int-ANG II) together with either candesartan, nimodipine or spironolactone or for aldosterone alone. No significant changes over time were noted.

DISCUSSION

The essential result of the present study is that ANG II was demonstrated to cause a direct, rapid, dose-dependent, and partly reversible increase in the glomerular permeability to macromolecules in rats in vivo. These changes in permeability could be completely abrogated by the ANG II receptor blocker candesartan but remained unchanged after inhibition of the hemodynamic actions of ANG II. Essentially, the response pattern of glomerular permeability following ANG II is similar to that seen after e.g., systemic infusions of atrial natriuretic peptide (ANP) (7) in rats. Thus there was an initial, large permeability increase, peaking at 5–15 min, which was largely reversible within the following 20 min, but followed by a more sustained and low-grade enhancement in glomerular permeability. The latter could be (partly) blocked by spironolactone.

The actions of ANG II on glomerular permeability and the antiproteinuric effects of ACEi and ARB have been a controversial issue over the last few decades. The predominant view has been that ACEi and ARB mainly affect glomerular hemodynamics to reduce the intracapillary hydrostatic pressure elevation induced by ANG II, thereby reducing the net filtration pressure, and hence, the transfer of proteins across the GFB. Furthermore, ANG II acts as a growth factor, driving interstitial fibrosis via cytokines, mainly transforming growth factor-β, in chronic kidney disease, which can be ameliorated by ACEi and ARB (10, 26). Although these actions are indeed crucial for the efficacy of RAAS inhibitors in the treatment of progressive renal disease and proteinuria, the present study demonstrates a direct, dynamic action of ANG II (and aldosterone) on the permeability of the GFB. Thus the antiproteinuric effects of ACEi or ARB may be partially dependent on their action to counteract the direct ANG II effects on the GFB.

The first evidence that the urinary albumin excretion may increase after the administration of renin was given by Pickering and Prinzmetal (35) in the rabbit. Eisenbach et al. (15), using a micropuncture technique in rats to collect proximal tubular fluid (PTF), found that systemic ANG II infusion (15 $ng \cdot min^{-1} \cdot 100$ g rat body wt^{-1}) caused a 26-fold increase in PTF albumin concentration (from a baseline value of 4.9 ± 3.0 mg/l), while single-nephron GFR did not change significantly. Furthermore, in the isolated, perfused rat kidney (IPK) ANG II, infused at a rate of 3 or 8 ng/min directly into the renal artery, induced a progressive and significant increase in urinary albumin excretion rate and in an enhanced filtration of Ficoll molecules of radii >34 Å (25). Later, it was demonstrated that a similar intrarenal infusion into the IPK of ANG II caused an increase in albumin permeability without any gross electron microscopic alterations of the morphology of the GFB (28) but that ANG II could induce a reorganization of the cellular F-actin filaments and a redistribution of zonula occludens-1 (ZO-1) in podocyte monolayers.

In a recent overview, the tentative action of ANG II on cellular Ca^{2+} influx to modulate the actin cytoskeleton in podocytes was reviewed (17). Very briefly, in a first step, ANG

Table 3. *Two-pore parameters at 15 and 120 min in Nim-Hi-Int-ANG II*

	Baseline	Nim-Hi-Int-ANG II 15 min	Nim-Hi-Int-ANG II 120 min
Small-pore radius (r_s), Å	45.1 ± 0.41	47.4 ± 0.35*	46.3 ± 0.35*
Large-pore radius (r_L), Å	130 ± 13.7	114 ± 12.3	130 ± 7.60
$\alpha_L \times 10^5$	3.71 ± 0.99	144 ± 51.4†	10.6 ± 0.75*
J_{vL}/GFR $\times 10^5$	9.46 ± 1.96	334 ± 118.4*	29.4 ± 1.77*
$A_0/\Delta X$, cm/g $\times 10^{-5}$	6.84 ± 0.64	5.83 ± 0.74	5.74 ± 0.43

Values are means ± SE. Nim, nimodipine; r_s, small-pore radius; Statistical differences between experimental groups and baseline: *$P < 0.05$, †$P < 0.01$.

Table 4. *Two-pore parameters at 15 and 120 min in Spir-Hi-Int-ANG II*

	Baseline	Spir-Hi-Int-ANG II 15 min	Spir-Hi-Int-ANG II 120 min
Small-pore radius (r_s), Å	44.7 ± 0.41	46.9 ± 0.21†	46.1 ± 0.25*
Large-pore radius (r_L), Å	121 ± 11.2	111 ± 9.59	106 ± 4.68
$\alpha_L \times 10^5$	3.36 ± 0.97	77.3 ± 21.7†	18.7 ± 6.39*
J_{vL}/GFR $\times 10^5$	9.01 ± 2.81	179 ± 46.0†	45.3 ± 16.2*
$A_0/\Delta X$, cm/g $\times 10^{-5}$	7.61 ± 0.32	6.69 ± 0.38	5.79 ± 0.25*

Values are means ± SE. Spir, spironolactone. Statistical differences between experimental groups and baseline: *$P < 0.05$, †$P < 0.01$.

II binds to its receptor (AT1R), which subsequently activates the transient receptor potential canonical (TRPC) channels, TRPC5, and, to a minor extent, TRPC6, which results in Ca^{2+} influx into the cell. It was hypothesized that TRPC5-driven signaling may be predominant under pathological conditions of excess ANG II and may lead to an increased activity of preferentially the small GTPase Rac1. Next, the Ca^{2+}-activated phosphatase, calcineurin, or kinases, such as PKA, compete for downstream effects on synaptopodin, mainly a target of calcineurin, and NFAT, mainly a target of PKA. At the next level, the small GTPases Rac1, RhoA, and Cdc42 compete for downstream effects on the actin cytoskeleton. Inhibition of Rac1 apparently has antiproteinuric effects, presumably because it seems to decrease the activity of the mineralocorticoid receptor (MR), while stimulation of Rac1 may lead to insertion of TRPC5 channels in the plasma membrane, further amplifying the ANG II signaling effects in a positive feedback loop (45). It was thus hypothesized that in states of excess ANG II, TRPC5/Rac1 overactivity may drive proteinuria. Under physiological conditions, however, active TRPC6 channels seem to be more abundant in the podocyte cell membrane than TRPC5 (47).

The rationale for ANG II to increase the permeability of the GFB is obscure. All the components of the RAAS are actually found in the kidney, and ANG II can be formed locally (23, 24, 37). Thus there have been speculations that intrarenally formed ANG II may be even more important than circulating ANG II in controlling, for example, sodium excretion (16). An increased level of circulating ANG II, causing a transiently increased permeability of the GFB, may provide the tubules with more substrate (renin and angiotensinogen) for the production of intrarenally formed ANG II (30, 36). In the present study, the first permeability peak after ANG II was relatively short and may be regarded as distinct from the long-acting effects of ANG II on glomerular permeability. It may be speculated that the first permeability peak may be instrumental in boosting the activation of the intrarenal RAAS system and the local formation of ANG II, but this speculation warrants further investigation.

It was previously demonstrated from this group that anaphylaxis (5), acute hyperglycemia (6), or systemic ANP (7) infusions in rats can transiently open the GFB, similar to ANG II, conceivably by affecting the cells of the GFB, i.e., the podocytes and the endothelium. Podocytes may indeed be the culprit in this context. Although there is good evidence that the ultimate sieving barrier to proteins is not at the podocyte level (27, 40), podocyte interactions with the rest of the GFB apparently are crucial for its integrity. Podocytes interact with the glomerular basement membrane (GBM) by integrins and seem to "pressurize" the GBM by its contractile nature in an adaptive way to resist any detrimental effects induced by increases in glomerular hydrostatic capillary pressure (17, 19). Thus changes in podocyte cell actin dynamics may directly affect the uphill components of the GFB. Also, ANG II receptors (AT1R) are present in endothelial cells, and direct effects on the endothelium cannot be excluded. Indeed, endothelial cells can react to e.g., histamine, substance P, or thrombin with contraction, to open paracellular gaps, with a time cycle very similar to that shown for the (first) permeability peak in the present experiments (18, 29).

Aldosterone is thought to act on the distal nephron to promote sodium reabsorption by initiating genomic events to increase transepithelial electrolyte transport. In contrast to this rather slow process, it has in recent years become apparent that aldosterone, like other steroids, is able to evoke rapid (non-

Table 5. *MAP, HR and hematocrit in Aldo, Cand-Hi-Int-ANG II, Nim-Hi-Int-ANG II, and Spir-Hi-Int-ANG II*

	Baseline	5 min	15 min	30 min	60 min	120 min
Aldo, $n = 7$						
Hct %	47.9 ± 0.8	47.5 ± 0.8	46.7 ± 0.7	46.8 ± 0.7	46.5 ± 0.5	46.2 ± 0.7
MAP, mmHg	117 ± 4.1	117 ± 3.9	115 ± 4.2	112 ± 2.8	110 ± 3.6	110 ± 4.3
HR, beats/min	367 ± 17	365 ± 15	357 ± 19	342 ± 23	340 ± 20	340 ± 18
Cand-Hi-Int-ANG II, $n = 6$						
Hct, %	47.5 ± 0.7		47.5 ± 0.9	47.0 ± 0.6		
MAP, mmHg	120 ± 4.2		115 ± 5.4	116 ± 6.8		
HR, beats/min	378 ± 10		378 ± 11	372 ± 12		
Nim-Hi-Int-ANG II, $n = 6$						
Hct, %	47.5 ± 0.9	48.7 ± 0.8	49.2 ± 0.7	49.4 ± 0.8	48.9 ± 0.6	47.9 ± 0.8
MAP, mmHg	111 ± 1.3	111 ± 2.5	109 ± 2.9	109 ± 2.8	110 ± 2.3	110 ± 1.5
HR, beats/min	374 ± 14	394 ± 8	396 ± 6	388 ± 11	382 ± 11	370 ± 11
Spir-Hi-Int-ANG II, $n = 7$						
Hct, %	49.7 ± 0.6	49.2 ± 1.3	50.2 ± 0.7	50.3 ± 0.6	50.4 ± 0.7	49.9 ± 0.7
MAP, mmHg	113 ± 3.6	144 ± 2.4*	144 ± 3.8*	142 ± 2.5*	141 ± 3.7*	142 ± 4.1*
HR, beats/min	360 ± 9	372 ± 11	368 ± 11	358 ± 8	362 ± 12	350 ± 14

Values are means ± SE. Aldo, aldosterone; Cand, candesarten. Statistical differences between experimental groups and baseline: *$P < 0.01$.

Table 6. *Log-normal distributed+shunt model, Lo-ANG II, and Hi-Int-ANG II*

	Baseline	Lo-ANG II 15 min	Lo-ANG II 120 min	Hi-Int-ANG II 15 min	Hi-Int-ANG II 120 min
Pore radius (u), Å	34.7 ± 0.79	33.5 ± 1.04	32.1 ± 1.17	28.1 ± 0.9*	30.8 ± 0.39*
Distribution spread (s)	1.15 ± 0.008	1.16 ± 0.01	1.18 ± 0.01	1.25 ± 0.02*	1.21 ± 0.004*
$A_0/\Delta X$, cm/g × 10^{-5}	38.7 ± 5.48	44.4 ± 4.99	44.8 ± 3.57	56.9 ± 23.1	53.9 ± 4.99
Shunt × 10^5 (Jv_{shunt}/GFR)	4.37 ± 0.78	13.8 ± 4.93	4.42 ± 1.62	24.6 ± 8.47*	17.9 ± 6.65

Values are means ± SE. Baseline data are pooled for all groups. u, Pore radius, Å; s, distribution spread of the pore radius. Statistical differences between experimental groups and baseline: *$P < 0.01$.

genomic) responses in various cells, such as in vascular smooth muscle cells and endothelial cells (43). Podocytes have mineralocorticoid receptors (MR), and, as mentioned above, Rac1 inhibition has been shown to have an antiproteinuric effect in vivo by decreasing the activity of MR. In the present study, aldosterone produced a rapid and marked increase in permeability, similar to that induced by ANG II (Lo-ANG II). Since aldosterone is released from the adrenal cortex following systemic ANG II infusion (after just a few minutes), part of the initial permeability enhancement during ANG II infusion may be due to aldosterone. However, pretreating the animals with spironolactone, an aldosterone antagonist, before the infusion of high doses of ANG II did not affect the permeability changes recorded at 15 and 30 min after the start of the ANG II infusion, while there were significant effects at 60 and 120 min (and 5 min) after the start of the ANG II infusion. Thus we cannot completely rule out that some of the permeability increases induced by ANG II may actually be dependent on aldosterone. This was especially evident for the sustained actions of ANG II. Anyway, the present experiments were performed to assess the systemic effects of ANG II on the GFB, in which aldosterone indeed plays a part.

According to the two-pore model, and similar to the glomerular permeability changes seen previously in anaphylactic shock, during acute hyperglycemia, or after ANP infusion in rats (5–7), the observed permeability changes following low doses of ANG II (Lo-ANG II) could be ascribed to an increased number of functional large pores in the GFB, without any significant changes in the small-pore pathway. However, the highest ANG II doses tested (especially Hi-Int-ANG II and Hi-ANG II, respectively), in addition caused alterations in the small-pore system, with an increased "breadth" of the pore distribution according to the log-normal distributed pore model. This is a permeability pattern that can be seen for very marked increases in glomerular permeability, such as in PAN nephrotic syndrome (20), but as mentioned above, such alterations have also been recorded for high doses of ANG II given to the isolated, perfused kidney (13, 25). At present, it is not known whether this is a general phenomenon occurring whenever very large increases in the permeability of the GFB are induced, or whether these changes may be specific to ANG II when infused at high concentrations.

In several previous studies, we have assessed θ for albumin using a tissue uptake technique in parallel with the determinations of θ to FITC-Ficoll (3, 4). The tissue uptake technique employed to assess θ for albumin requires that a free label (^{125}I) is less than ~0.1% of total tracer radioactivity, which, unfortunately, could not be obtained in the present study. In a preliminary study, it turned out that θ for albumin got markedly overestimated during control conditions due to high levels of denaturated protein and free iodine (^{125}I). However, since we have found a near complete coupling between alterations in θ for albumin with that for high-molecular-weight Ficoll molecules ($Ficoll_{50-80Å}$) during conditions of increased permeability, we consider it quite safe to rely upon the glomerular θ to high molecular weight Ficoll ($Ficoll_{50-80Å}$) as an indicator of glomerular permeability. Indeed, $Ficoll_{55Å}$ has been reported to be a very good surrogate marker for native (negatively charged) albumin in this context (19, 31).

In summary, the present study is the first to describe in detail the dynamic, time-dependent actions of ANG II on the permeability of the GFB to macromolecules. Thus there was a dose-dependent, rapid, partly reversible increase in glomerular permeability, peaking at 5–15 min, which could be completely abrogated by the ANG II blocker candesartan. After the first permeability peak, glomerular permeability was partly reversed, but some elevations in permeability remained even after 60 and 120 min, which could be (partly) blocked by spironolactone. The actions of ANG II on the GFB occurred independently from its hemodynamic actions, since the total elimination of ANG II hemodynamics by an L-type Ca^{2+} channel blocker did not reduce the permeability increases observed. According to a two-pore model and a log-normal distributed pore model, ANG II caused increases in glomerular permeability due to the formation of an increased number of large pores of the glomerular filter, and, at high doses, also an increase in the dispersity of the small-pore radius. The present data have implications for understanding the effects of ACEi/ARB on glomerular proteinuria, where at least part of the antiproteinuric effects of these agents seem to be dependent on their action to counteract the direct effects of ANG II on the permeability of the GFB.

APPENDIX I

Log-Normal Distributed+Shunt Model

A log-normal distributed pore model according to Axelsson et al. (8) was used to describe the experimental data. The model is a nonlinear variant of the distributed two-pore model presented by Arturson et al. (2) using the Patlak equation (33) instead of the molecular sieving theory developed by Pappenheimer et al. (32). In addition, the "large-pore" pathway is replaced by a shunt. The definitions of constants and hydrodynamic estimates are essentially the same as those used in the two-pore model according to Rippe and Haraldsson (39). The model assumes that the glomerular filtration barrier has a log-normal distributed array, g (r, u, s), of pores

$$g(r,u,s) = \frac{1}{\sqrt{2\pi}r\ln s}e^{-\frac{1}{2}\left(\frac{\ln r - \ln u}{\ln s}\right)^2} \quad (1)$$

where u is the average (distributed) pore radius and s is the "distribution parameter," and where $f_H = Jv_H/Jv$, i.e., the fractional fluid flow through restrictive pores (with a distributed radius) in parallel

with an unselective shunt, f_L. Here ($f_L = 1 - f_H$). Hence, the total fractional clearance is given by

$$\theta = f_H\theta_H + f_L \quad (2)$$

where θ_H is the fractional clearance generated by the distributed pores according to the well-known equation

$$\theta_H = \frac{1-\sigma}{1-\sigma e^{-Pe}} \quad (3)$$

As with any model based upon this equation, at least three parameters must be determined: the permeability-surface area product, *PS*, the reflection coefficient, σ, and the hydraulic conductivity, $K_f = L_pS$, or total cross-sectional pore area, A_0, for each type/size of pathway. The fractional contribution of all the pore sizes in the distribution to the final area, A_i, is an intrinsic property of any heteroporous barrier with a discrete pore size distribution [$A_i = \alpha_1\pi(r_1)^2 + \alpha_2\pi(r_2)^2 + \ldots + \alpha_n\pi(r_n)^2$], or a continuous pore-size distribution and is given by

$$A_i = \int_0^\infty \pi r^2 g(r)\mathrm{d}r \quad (4)$$

Since the fractional surface area accounted for pores in the distribution of radius *R* is

$$A_f = \pi R^2 g(R) \quad (5)$$

the total *PS* for the entire barrier is calculated by integrating overall pore radii in the distribution

$$PS = D_s\frac{A_0}{\Delta x}\int_0^\infty \frac{A_f}{A_i}\frac{A}{A_0}\mathrm{d}r = \frac{\int_0^\infty D_s\frac{A_0}{\Delta x}\frac{A}{A_0}r^2 g(r)\mathrm{d}r}{\int_0^\infty r^2 g(r)\mathrm{d}r} \quad (6)$$

Using a similar argument, it can be shown that the total reflection coefficient is

$$\sigma = \frac{\int_0^\infty r^4 g(r)\sigma_h(r)\mathrm{d}r}{\int_0^\infty r^4 g(r)\mathrm{d}r} \quad (7)$$

Optimal values for *u*, *s*, $A_0/\Delta X$ and f_L were calculated using the nonlinear regression method of Levenberg and Marquardt using the well-known MINPACK software library with standard settings.

ACKNOWLEDGMENTS

Kerstin Wihlborg is greatly acknowledged for skillful typing of the manuscript.

GRANTS

This study was supported by the Swedish Research Council (Grant 08285), the Heart and Lung Foundation, and the Medical Faculty at Lund University (ALF Grant).

DISCLOSURES

No conflicts of interest, financial or otherwise, are declared by the authors.

AUTHOR CONTRIBUTIONS

Author contributions: J.A. and B.R. provided conception and design of research; J.A. and A.R. performed experiments; J.A., A.R., and C.M.Ö. analyzed data; J.A., A.R., C.M.Ö., and B.R. interpreted results of experiments; J.A. prepared figures; J.A. and B.R. drafted manuscript; J.A., A.R., C.M.Ö, and B.R. edited and revised manuscript; J.A., A.R., C.M.Ö., and B.R. approved final version of manuscript.

REFERENCES

1. **Andrews PM, Coffey AK.** Cytoplasmic contractile elements in glomerular cells. *Federation Proc* 42: 3046–3052, 1983.
2. **Arturson G, Groth T, Grotte G.** Human glomerular membrane porosity and filtration pressure: dextran clearance data analysed by theoretical models. *Clin Sci* 40: 137–158, 1971.
3. **Asgeirsson D, Venturoli D, Rippe B, Rippe C.** Increased glomerular permeability to negatively charged Ficoll relative to neutral Ficoll in rats. *Am J Physiol Renal Physiol* 291: F1083–F1089, 2006.
4. **Axelsson J, Mahmutovic I, Rippe A, Rippe B.** Loss of size selectivity of the glomerular filtration barrier in rats following laparotomy and muscle trauma. *Am J Physiol Renal Physiol* 297: F577–F582, 2009.
5. **Axelsson J, Rippe A, Venturoli D, Swärd P, Rippe B.** Effects of early endotoxemia and dextran-induced anaphylaxis on the size selectivity of the glomerular filtration barrier in rats. *Am J Physiol Renal Physiol* 296: F242–F248, 2009.
6. **Axelsson J, Rippe A, Rippe B.** Acute hyperglycemia induces rapid, reversible increases in glomerular permeability in nondiabetic rats. *Am J Physiol Renal Physiol* 298: F1306–F1312, 2010.
7. **Axelsson J, Rippe A, Rippe B.** Transient and sustained increases in glomerular permeability following ANP infusion in rats. *Am J Physiol Renal Physiol* 300: F24–F30, 2011.
8. **Axelsson J, Öberg C, Rippe A, Krause B, Rippe B.** Size-selectivity of a synthetic high-flux and a high cut-off dialyzing membrane compared to that of the rat glomerular filtration barrier. *J Membr Sci* 413–414: F29–F37, 2012.
9. **Bohrer MP, Deen WM, Robertson CR, Brenner BM.** Mechanism of angiotensin II-induced proteinuria in the rat. *Am J Physiol Renal Fluid Electrolyte Physiol* 233: F13–F21, 1977.
10. **Brenner BM, Cooper ME, de Zeeuw D, Keane WF, Mitch WE, Parving HH, Remuzzi G, Snapinn SM, Zhang Z, Shahinfar S.** Effects of losartan on renal and cardiovascular outcomes in patients with type 2 diabetes and nephropathy. *N Engl J Med* 345: 861–869, 2001.
11. **Brown AJ, Casals-Stenzel J, Gofford S, Lever AF, Morton JJ.** Comparison of fast and slow pressor effects of angiotensin II in the conscious rat. *Am J Physiol Heart Circ Physiol* 241: H381–H388, 1981.
12. **Christensen EI, Birn H, Rippe B, Maunsbach AB.** Controversies in nephrology: renal albumin handling, facts, and artifacts! *Kidney Int* 72: 1192–1194, 2007.
13. **Clavant SP, Forbes JM, Thallas V, Osicka TM, Jerums G, Comper WD.** Reversible angiotensin II-mediated albuminuria in rat kidneys is dynamically associated with cytoskeletal organization. *Nephron Physiol* 93: p51–p60, 2003.
14. **Comper WD, Haraldsson B, Deen WM.** Resolved: normal glomeruli filter nephrotic levels of albumin. *J Am Soc Nephrol* 19: 427–432, 2008.
15. **Eisenbach GM, Liew JB, Boylan JW, Manz N, Muir P.** Effect of angiotensin on the filtration of protein in the rat kidney: a micropuncture study. *Kidney Int* 8: 80–87, 1975.
16. **Gonzalez-Villalobos RA, Billet S, Kim C, Satou R, Fuchs S, Bernstein KE, Navar LG.** Intrarenal angiotensin-converting enzyme induces hypertension in response to angiotensin I infusion. *J Am Soc Nephrol* 22: 449–459, 2011.
17. **Greka A, Mundel P.** Balancing calcium signals through TRPC5 and TRPC6 in podocytes. *J Am Soc Nephrol* 22: 1969–1980, 2011.
18. **Haraldsson B, Zackrisson U, Rippe B.** Calcium dependence of histamine-induced increases in capillary permeability, studied in isolated rat hindlimbs. *Acta Physiol Scand* 128: 247–258, 1986.
19. **Haraldsson B, Nyström J, Deen WM.** Properties of the glomerular barrier and mechanisms of proteinuria. *Physiol Rev* 88: 451–487, 2008.
20. **Hjalmarsson C, Ohlson M, Haraldsson B.** Puromycin aminonucleoside damages the glomerular size barrier with minimal effects on charge density. *Am J Physiol Renal Physiol* 281: F503–F512, 2001.
21. **Hollenberg NK, Chenitz WR, Adams DF, Williams GH.** Reciprocal influence of salt intake on adrenal glomerulosa and renal vascular responses to angiotensin II in normal man. *J Clin Invest* 54: 34–42, 1974.
22. **Hsu HH, Hoffmann S, Endlich N, Velic A, Schwab A, Weide T, Schlatter E, Pavenstadt H.** Mechanisms of angiotensin II signaling on cytoskeleton of podocytes. *J Mol Med (Berl)* 86: 1379–1394, 2008.
23. **Inagami T, Kawamura M, Naruse K, Okamura T.** Localization of components of the renin-angiotensin system within the kidney. *Federation Proc* 45: 1414–1419, 1986.
24. **Ingelfinger JR, Zuo WM, Fon EA, Ellison KE, Dzau VJ.** In situ hybridization evidence for angiotensinogen messenger RNA in the rat proximal tubule. An hypothesis for the intrarenal renin angiotensin system. *J Clin Invest* 85: 417–423, 1990.

25. **Lapinski R, Perico N, Remuzzi A, Sangalli F, Benigni A, Remuzzi G.** Angiotensin II modulates glomerular capillary permselectivity in rat isolated perfused kidney. *J Am Soc Nephrol* 7: 653–660, 1996.
26. **Lewis EJ, Hunsicker LG, Bain RP, Rohde RD.** The effect of angiotensin-converting-enzyme inhibition on diabetic nephropathy. The Collaborative Study Group. *N Engl J Med* 329: 1456–1462, 1993.
27. **Lund U, Rippe A, Venturoli D, Tenstad O, Grubb A, Rippe B.** Glomerular filtration rate dependence of sieving of albumin and some neutral proteins in rat kidneys. *Am J Physiol Renal Physiol* 284: F1226–F1234, 2003.
28. **Macconi D, Abbate M, Morigi M, Angioletti S, Mister M, Buelli S, Bonomelli M, Mundel P, Endlich K, Remuzzi A, Remuzzi G.** Permselective dysfunction of podocyte-podocyte contact upon angiotensin II unravels the molecular target for renoprotective intervention. *Am J Pathol* 168: 1073–1085, 2006.
29. **McDonald DM.** Endothelial gaps and permeability of venules in rat tracheas exposed to inflammatory stimuli. *Am J Physiol Lung Cell Mol Physiol* 266: L61–L83, 1994.
30. **Navar LG, Prieto MC, Satou R, Kobori H.** Intrarenal angiotensin II and its contribution to the genesis of chronic hypertension. *Curr Opin Pharmacol* 11: 180–186, 2011.
31. **Ohlson M, Sörensson J, Lindström K, Blom AM, Fries E, Haraldsson B.** Effects of filtration rate on the glomerular barrier and clearance of four differently shaped molecules. *Am J Physiol Renal Physiol* 281: F103–F113, 2001.

31a. **Palm F.** The dark side of angiotensin II: direct dynamic regulation of the glomerular filtration barrier permeability to macromolecules. Focus on "Rapid, dynamic changes in glomerular permeability to macromolecules during systemic angiotensin II (ANG II) infusion in rats." *Am J Physiol Renal Physiol* (June 20, 2012). doi:10.1152/ajprenal.00153.2012.

32. **Pappenheimer JR, Renkin EM, Borrero LM.** Filtration, diffusion and molecular sieving through peripheral capillary membranes. A contribution to the pore theory of capillary permeability. *Am J Physiol* 167: 13–46, 1951.
33. **Patlak CS, Goldstein DA, Hoffman JF.** The flow of solute and solvent across a two-membrane system. *J Theor Biol* 5: 426–442, 1963.
34. **Peti-Peterdi J, Sipos A.** A high-powered view of the filtration barrier. *J Am Soc Nephrol* 21: 1835–1841, 2010.
35. **Pickering GW, Prinzmetal M.** The effect of renin on urine formation. *J Physiol* 98: 314–335, 1940.
36. **Pohl M, Kaminski H, Castrop H, Bader M, Himmerkus N, Bleich M, Bachmann S, Theilig F.** Intrarenal renin angiotensin system revisited: role of megalin-dependent endocytosis along the proximal nephron. *J Biol Chem* 285: 41935–41946, 2010.
37. **Pratt RE, Zou WM, Naftilan AJ, Ingelfinger JR, Dzau VJ.** Altered sodium regulation of renal angiotensinogen mRNA in the spontaneously hypertensive rat. *Am J Physiol Renal Fluid Electrolyte Physiol* 256: F469–F474, 1989.
38. **Rad AK, Balment RJ, Ashton N.** Rapid natriuretic action of aldosterone in the rat. *J Appl Physiol* 98: 423–428, 2005.
39. **Rippe B, Haraldsson B.** Transport of macromolecules across microvascular walls. The two-pore theory. *Physiol Rev* 74: 163–219, 1994.
40. **Rippe C, Asgeirsson D, Venturoli D, Rippe A, Rippe B.** Effects of glomerular filtration rate on Ficoll sieving coefficients (theta) in rats. *Kidney Int* 69: 1326–1332, 2006.
41. **Russo L, Bakris GL, Comper WD.** Renal handling of albumin: a critical review of basic concepts and perspective. *Am J Kidney Dis* 39: 899–919, 2002.
42. **Saleem MA, Zavadil J, Bailly M, McGee K, Witherden IR, Pavenstadt H, Hsu H, Sanday J, Satchell SC, Lennon R, Ni L, Bottinger EP, Mundel P, Mathieson PW.** The molecular and functional phenotype of glomerular podocytes reveals key features of contractile smooth muscle cells. *Am J Physiol Renal Physiol* 295: F959–F970, 2008.
43. **Schneider M, Ulsenheimer A, Christ M, Wehling M.** Nongenomic effects of aldosterone on intracellular calcium in porcine endothelial cells. *Am J Physiol Endocrinol Metab* 272: E616–E620, 1997.
44. **Sharma R, Lovell HB, Wiegmann TB, Savin VJ.** Vasoactive substances induce cytoskeletal changes in cultured rat glomerular epithelial cells. *J Am Soc Nephrol* 3: 1131–1138, 1992.
45. **Shibata S, Nagase M, Yoshida S, Kawarazaki W, Kurihara H, Tanaka H, Miyoshi J, Takai Y, Fujita T.** Modification of mineralocorticoid receptor function by Rac1 GTPase: implication in proteinuric kidney disease. *Nat Med* 14: 1370–1376, 2008.
46. **Tanner G, Rippe C, Shao Y, Evan AP, Williams JC Jr.** Glomerular permeability to macromolecules in the *Necturus* kidney. *Am J Physiol Renal Physiol* 296: F1269–F1278, 2009.
47. **Tian D, Jacobo SM, Billing D, Rozkalne A, Gage SD, Anagnostou T, Pavenstadt H, Hsu HH, Schlondorff J, Ramos A, Greka A.** Antagonistic regulation of actin dynamics and cell motility by TRPC5 and TRPC6 channels. *Sci Signal* 3: ra77, 2010.
48. **Tojo A, Endou H.** Intrarenal handling of proteins in rats using fractional micropuncture technique. *Am J Physiol Renal Fluid Electrolyte Physiol* 263: F601–F606, 1992.